Generation of highly uniform droplets using asymmetric microchannels fabricated on a single crystal silicon plate: effect of emulsifier and oil types

Goran T. Vladisavljević[1†], Isao Kobayashi[2], Mitsutoshi Nakajima[2,3]

[1]*Chemical Engineering Department, Loughborough University, Loughborough, Leicestershire, LE11 3TU, UK*

[2]*Food Engineering Division, National Food Research Institute, Kannondai 2-1-12, Tsukuba, Ibaraki 305-8642, Japan*

[3]*Graduate School of Life and Environmental Sciences, University of Tsukuba, Tennoudai 1-1-1, Tsukuba, Ibaraki 305-8572, Japan*

[†]Corresponding author: Phone: + 44 (0) 1509 222 518; Fax: + 44 (0) 1509 223 923; E-mail address: G.Vladisavljevic@lboro.ac.uk

Abstract

Uniform droplets of soybean oil, MCT (medium-chain fatty acid triglyceride) oil and n-tetradecane with a mean diameter of 26-29 μm have been generated using a silicon 24 × 24 mm microchip consisting of 23,489 asymmetric microchannels fabricated by photolitography and deep reactive ion etching. Each microchannel consisted of a circular 10-μm diameter straight hole with a length of 70 μm and a 50 × 10 μm rectangular microslot with a depth of 30 μm. At the constant oil flux of 10 $Lm^{-2}h^{-1}$, the percent of active channels increased with increasing the oil viscosity and ranged from 4 % for n-tetradecane to 48 % for soybean oil. The size distribution

span for SDS (sodium sodium dodecyl sulphate)- and Tween 20 (polyoxyethylene (20) sorbitan monolaurate)-stabilised soybean and MCT oil droplets was 0.21-022. The ability of asymmetric microchannels to generate monodisperse soybean oil droplets at the very low SDS concentration of 0.01 wt% has been demonstrated. At the SDS concentration below the CMC, the generated droplets tend to attach to the plate surface, whereas at the higher SDS concentration they detach from the plate as soon as they are formed. The agreement between the experimental and CFD (Computational Fluid Dynamics) simulation results was excellent for soybean oil and the poorest for n-tetradecane.

Keywords: Microchannel emulsification; Silicon microchip; Droplet generation; Monodisperse droplets; Asymmetric microchannel plate.

1. Introduction

A microfluidic device can be identified by the fact that it has one or more channels with at least one dimension less than 1 mm. The most common types of microfluidic devices are: (i) soft microfluidic devices fabricated by soft lithography in elastomeric materials such as poly(dimethyl siloxane) (PDMS) [1], (ii) microfluidic glass devices manufactured by etching or micromachining in quartz glass or glassy polymers such as poly(methyl methacrylate) (PMMA) [2], and (iii) microchannel (MC) array devices fabricated in single crystal silicon by photolithography and wet-etching or deep-reactive ion etching processing [3]. Microfluidic T-junctions and flow focusing devices can generate monodispersed droplets with a coefficient of variation in the dripping regime of generally less than 3 %. Although the frequency of droplet generation can be as high as 12,000 Hz for water-in-oil droplets [4], the throughput in terms of

volume flow rate of the disperse phase is very low because the droplets are formed from a single microchannel. These microfluidic devices are investigated for capillary electrophoresis [5], immunoassays [6], cellomics [7], proteomics [8], DNA analysis [9], etc.

Microchannel array devices are much more suitable for larger-scale applications, because in these devices the droplets are simultaneously formed from hundreds or even hundreds of thousands [10] of microchannels. The monodispersed droplets produced by MC emulsification have been subjected to various secondary processes/reactions (gelation, polymerisation, crystallisation) to form solid microparticles such as polymer microspheres [11, 12], gel microbeads [13, 14], and solid lipid microparticles [15, 16]. Other complex microstructures with a controlled size distribution have also been created using this technique such as gelatin/acacia complex coacervate microcapsules [17], microbubbles [18], giant vesicles [19], discoid droplets [20], surfactant-free droplets stabilized by silica nanoparticles [21], gel beads containing living cells [22], etc. The advantages of using this technique are high entrapment efficiency of encapsulated species and close control of particle size in addition to much greater droplet productivity than that achievable in T-junctions or flow focusing devices.

The MC arrays can be fabricated horizontal to the plate surface as open microgrooves [3] or vertical to the plate surface as straight through holes [23]. The grooved silicon MC plates for blood rheology measurements have been developed by Kikuchi et al. [24] and adopted for droplet generation by Kawakatsu et al. [3]. The grooved MC plates exhibit a low droplet productivity of generally less than 0.1 mLh^{-1}, due to limited number of channels (100 - 1500). The 'straight-through' MC plates developed by Kobayashi et al. [23] consist of several thousands to several hundreds of thousands of MCs and have a maximum droplet productivity in the dripping regime of 50 mLh^{-1} or even more with a coefficient of variation less than 5 %, estimated using an image analysis software. A straight-through MC plate can be symmetric or asymmetric in structure, as

shown in Figure 1. The symmetric structure of a MC plate implies that the channels are of the same size and geometry over the whole cross section of the plate, i.e. either rectangular (Fig. 1(a)) or circular (Fig 1(b)) [23, 25-27]. According to Kobayashi et al. [28], rectangular microslots provide better droplet monodispersity than circular microchannels and a slot aspect ratio (length/width ratio) should be higher than 3 to obtain monodisperse droplets with a coefficient of variation smaller than 2 %.

The aim of this work was to investigate the generation of highly uniform droplets using novel asymmetric straight-through MC plate recently developed by Kobayashi et al. [29]. As shown in Figure 1(c), the asymmetric plate represents a hybrid between the two MC plates shown in Figures 1(a) and 1(b), with circular channels at the bottom side of the plate and rectangular slots at the top side. This structure is believed to provide an optimal geometry for creation of monodispersed droplets at high generation rates. Monodisperse droplets are advantageous both in fundamental investigations and practical applications. Emulsion appearance and rheology, stability against Oswald ripening and creaming, and the suitability of droplets as templates for manufacturing solid micro/nano-particles are strongly influenced by their particle size distribution.

2. Experimental

2.1 Silicon chip

The experiments have been carried out using silicon 24 × 24 mm MC plates (EP. Tech Co., Ltd., Hitachi, Japan, model WMS1-3) containing 23,489 MCs arranged within a 10 × 10 mm

central region. As shown in Fig. 2 (a), the plate was 500 μm thick, but it was thinned down to thickness 100 μm in the central region. The holes at the four corners of the plate permit a disperse phase to flow beneath the plate, as shown in Figure 3. The plate was microfabricated by photolithography and deep reactive ion etching (DRIE). Each MC consists of a circular 10-μm diameter straight hole with a depth of 70 μm and a 50 × 10 μm microslot (an aspect ratio = 5) with a depth of 30 μm (Table 1). The distance between the centres of the two adjacent channels in a row was 70 μm and the distance between the centres of the channels in the two adjacent rows was 60 μm (Figure 2(c)). Before first usage, the MC plate was subjected to plasma oxidation in a plasma reactor (PR41, Yamato Science Co. Ltd., Tokyo, Japan) to form a hydrophilic silicon dioxide layer on the surface. After each experiment the plate was cleaned in an ultrasound water bath (VS-100 III, As One Co., Osaka, Japan) using a commercial neutral detergent solution and stored immersed in 0.1 M nitric acid solution to maintain its strong hydrophilic nature.

2.2 Chemicals

2 wt% Tween 20 (polyoxyethylene (20) sorbitan monolaurate) or 0.01-2 wt% SDS (sodium dodecyl sulphate) dissolved in Milli Q water was used as a continuous phase in oil-in-water (O/W) emulsions. Both emulsifiers were purchased from Wako Pure Chemical Industries, Ltd, Osaka, Japan. The disperse phase was soybean oil, MCT (medium-chain fatty acid triglyceride) oil or n-tetradecane with a viscosity at 293 K of 50, 20, and 2.7 mPa·s, respectively (Table 2). Most naturally occurring fats are triglycerides - tri meaning that each molecule have three carbon chains. In the MCT oils each chain has 6 - 12 carbon atoms, and for the medically refined grades of MCT oil each chain has 8 - 10 carbon atoms. The MCT oil used in this work

was supplied by Taiyo Kagaku Co. Ltd, Yokkaishi, Japan, while soybean oil and n-tetradecane were purchased from Wako Pure Chemical Industries, Ltd (Osaka, Japan).

2.3 Experimental procedure

Prior to each experiment, the MC plate was degassed in the continuous phase by ultrasound treatment for 20 min. The dispersed phase was injected through the channels by a syringe pump (Harvard Apparatus, model 11 Plus) at the flow rate of 1 mLh^{-1} using a 5 mL glass syringe. This oil flow rate was equivalent to the flux value of 10 $Lm^{-2}h^{-1}$. The droplets were formed at the outlets of the microslots and swept away from the plate surface by a continuous phase flow. The flow rate of continuous phase was kept constant at 50 mL/h by another syringe pump using a 50 mL glass syringe. Therefore, the disperse phase content in the exit emulsion stream was approximately 2 vol %. The droplet generation was observed and recorded in real time using a high-resolution color CCD camera (LCL-211H, Watec America Corp. USA) attached to a microscope (MS-511-M; Seiwa Optical Co., Ltd., Tokyo, Japan) and a PC computer (Figure 3). The droplet generated rate was estimated from the high-speed video clips recorded using a Rabitt mini 2 camera (Photoron, Tokyo), that can provide images at up to 600 frames per second. The particle size distribution of the resultant emulsion droplets was measured using a commercial light scattering instrument (Beckman Coulter LS 13 320, Miami, FL). This instrument incorporates PIDS (Polarization Intensity Differential Scattering) technology to provide a size range that spans from 0.04 to 2000 μm.

3. Results and discussion

3.1 Effect of emulsifier content in continuous aqueous phase

The effect of emulsifier (SDS) content in the continuous phase has been investigated over a wide concentration range between 0.01 and 2 wt% using soybean oil as a dispersed phase. As shown in Figures 4 and 5, irrespective of the SDS concentration monodisperse emulsion droplets were obtained with a span of particle size distribution typically in the range of 0.210-0.225 [span = $d_{50}/(d_{90}-d_{10})$], although a very low span value of 0.087 was obtained at 0.5 wt%, as can be seen in Figure 5. Due to the high degree of monodispersity, the droplets spontaneously arranged themselves in regular 2D arrays as shown in Figure 6. Over the range of SDS concentration of 0.2-0.5 wt%, a coefficient of variation was 3-4 % estimated using the WinRoof image analysis software (Mitani Co., Fukui, Japan). In flow focusing microfluidic devices, the droplets are formed in a single microfluidic channel and a coefficient of variation is typically less than 3 % [30] or even less than 1 % [31].

The highest span value of 0.225 ± 0.007 has been found at 0.01 wt% SDS. However, even at this very low SDS content which is well below the critical micelle concentration of SDS in pure water of 0.2-0.25 wt%, the generated droplets were highly uniform in size, which could be explained by the presence of surface-active agents in soybean oil, such as free fatty acids (e.g., linoleic acid) and the asymmetric structure of MCs that promotes formation of highly uniform droplets. In the experiments with very low SDS concentration (0.01-0.1 wt%), the following problems have been identified: (i) At the SDS concentration of 0.01 and 0.02 wt.%, the soybean oil droplets were not stable against coalescence during storage at room temperature and

coalescence occurred after several hours; (ii) A significant amount of droplets were kept attached to the plate surface after generation due to the high interfacial tension force that prevails over the tangential drag force generated by cross flow. The attachment of droplets on the plate surface in the vicinity of the channel outlets as shown in Figure 7(b) may result in undesirable steric hindrance effects and the decrease in monodispersity at the higher oil fluxes; (iii) At the low SDS concentration, a proportion of active channels showed large variations over the plate surface during the same experiment, as could be seen in Figure 8. It was also a consequence of pressure drop in continuous phase and was avoided in the experiments reported in the paragraph 3.2 by using an improved design of MC module.

Over the range of SDS concentration of 0.5-2 wt%, which was above the CMC, the mean droplet diameter $d_{3,2}$ was 26.3 μm and unaffected by the SDS concentration (Figure 5). The mean droplet/channel size ratio of 2.63 was smaller than the mean droplet/pore size ratio of 3.0 found in droplet formation from Shirasu Porous Glass (SPG) membrane within the same range of SDS concentration [32], but similar to the mean droplet/pore size ratios in membrane emulsification using asymmetric aluminium oxide membranes [33, 34]. The $d_{3,2}$ value of 26.3 μm is significantly smaller than the average droplet diameter of 39.1 μm reported in straight-through MC emulsification for the system containing 1 wt% SDS and soybean oil using a symmetric MC plate with 10 × 50 μm channels [25]. In the case of symmetric channels a growing droplet retain a spherical shape during droplet formation process with an ellipsoidal or circular neck inside the channel [35], whereas in the case of asymmetric channels, a growing droplet is deformed inside a microslot into an ellipsoidal disc-like shape which is energetically highly unfavorable. As a results, the tendency of dispersed phase to detach is stronger for asymmetric channels and smaller droplets are formed than using symmetric channels.

Over the range of SDS concentration of 0.01-0.1 wt% which is below the CMC, the mean droplet size increased by 8 % as the SDS concentration was reduced from 0.01 to 0.1 wt% (Figure 5), which was a consequence of the increased interfacial tension force. Above the CMC, however, small satellite droplets with the diameter of about 1 μm have been formed from some of the channels, as shown in Figure 9. As pointed out by Tan et al. [36], satellite droplets have been observed in many droplet generation devices [37-41] and their generation is a result of the imbalance of capillary forces during the break-off of primary droplet [36]. A typical volume of the satellite droplet is less than 1% of the parent drop [38]. Due to their small quantity, the presence of satellite droplets in our emulsions could not be detected using the Beckman Coulter particle size analyser. Although the generation of satellite droplets is normally regarded as a problem in microfluidic devices, Tan et al. [42] have suggested the exploitation of this mechanism to generate uniform monodispersed nanoparticles.

Therefore, the optimum SDS concentration in our experiments was in the range of 0.2-0.5 wt%, because the droplet coalescence can occur at the SDS concentrations less than 0.2 wt% and the satellite droplets can be generated at the SDS contents higher than 0.5 wt%.

3.2 Effect of oil viscosity

Table 3 shows the effects of oil type on the mean droplet size and monodispersity and the characteristics of the droplet generation for the system containing 2 wt% Tween 20 at the oil flux of 10 L $m^{-2}h^{-1}$ and continuous phase flow rate between 250 and 400 mL h^{-1}. The influence of continuous phase flow rate was negligible, because the average flow velocity of the continous phase in that case was in the order of several mm/s. Because the flow regime was laminar, a

parabolic velocity profile was established between the plate surface and the upper glass plate and the continuous phase velocity near the plate surface where the droplets were formed, had very low values. The mean frequency of droplet generation ν_{dg} was estimated from the high-speed camera video clips by considering at least 100 active channels on the plate surface and observing at least 10 consecutive droplets generated at each channel. The number of active channels, N, has been found from the mass balance equation for the oil flowing through the channels: $Q_d = N\nu_{dg}V_d$, where $Q_d = 1$ mLh^{-1} is the volume flow rate of the disperse phase (oil) controlled by the syringe pump and V_d is the mean droplet volume given by $d_{4,3}^3\pi/6$, where $d_{4,3}$ is the volume-weighted mean particle diameter. Therefore, N was calculated using the equation: $N = 6Q_d/(\nu_{dg}d_{4,3}^3\pi)$. The fraction of active channels is given by $k = N/N_0$, where $N_0 = 23{,}348$ is the total number of channels. In Fig. 10, the percent of active channels is plotted against the oil viscosity at the constant oil flow rate. The percent of active channels exponentially increased with increasing the oil viscosity, but it was counterbalanced by the higher frequency of droplet generation at the lower viscosity. It is important to note that the mean values of ν_{dg} are given in Table 3 and Figure 10. For example, for soybean oil the mean droplet generation frequency was 2.8 Hz, but the local ν_{dg} values for different active channels varied from 1 to 7 Hz. The coefficient of variation of the local ν_{dg} values in various experiments was in the range from 33 to 49 %.

The agreement between the experimental and CFD (Computational Fluid Dynamics) simulation data was excellent for soybean oil, but less satisfactory for n-tetradecane. The CFD results for n-tetradecane overestimated the frequency of droplet generation by 28 %, but the agreement was amazingly good for soybean oil with respect to both the frequency of droplet generation and droplet diameter [43]. A commercial CFD code (CFD-ACE+ version 2004) with a finite volume method was used to calculate the droplet generation rate from a single asymmetric

channel [43]. The droplet formation time predicted by CFD was very short (less than 0.135 s), so that the interfacial tension was supposed to be equal to the interfacial tension at the pure water/oil interface listed in Table 2, i.e. the mass transfer of emulsifier molecules to the interface was neglected due to the short time between the droplet appearance on the plate and detachment.

The mean velocity of oil inside the circular part of active channels was calculated using the equation: $U = 4Q_d /(Nd_{channel}^2\pi)$, where $d_{channel}$ is the diameter of circular channels. It is obvious that U is inversely proportional to the number of active channels and therefore, the highest oil velocity through the channels was estimated for n-tetradecane (Table 3). The measured mean Sauter diameter $d_{3,2}$ decreased with increasing the oil viscosity, which is consistent with CFD simulation results previously reported for symmetric MC plate [26]. A more viscous oil produced smaller droplets because of the decrease of oil velocity in active microchannels. It is important to note that the particle size distribution span for soybean and MCT oil droplets was significantly lower than that for the droplets generated using Shirasu Porous Glass (SPG) membrane (span = 0.25-0.45) [34, 44] or sintered alumina membrane (span = 0.42-0.56) [45]. The distribution span for n-tetradecane droplets was relatively high indicating a wide distribution, but at the higher fluxes the span values of around 0.25 were obtained (these results are not presented here).

4. Conclusions

Highly uniform droplets of soybean oil and MCT (medium-chain fatty acid triglyceride) oil with the size distribution span of 0.21-022 and the mean Sauter diameter of 26-29 μm have been generated using an asymmetric silicon MC plate consisting of 10 × 50 μm microslots combined with circular 10-μm diameter channels. At the constant flow rate of oil through the plate, the

mean frequency of droplet generation from the active channels increased with decreasing the oil viscosity and it was compensated by the larger number of active channels at the higher oil viscosity. We have demonstrated the ability of asymmetric MC plate to generate monodisperse soybean oil droplets at very low emulsifier (SDS) concentration of 0.01 wt%. At too low SDS concentrations, droplets tend to attach to the plate surface and form 2D clusters near the outlets of the channels, whereas at the SDS concentration above the CMC they detach from the plate as soon as they are formed. However, at the SDS concentration above 0.5 wt% there is a tendency for small satellite droplets to be formed at some of the channels. However, the amount of satellite droplets was very small, because the presence of these droplets could not be detected using the Coulter particle size analyser. The agreement between the experimental and CFD simulation results was excellent for soybean oil and the poorest for n-tetradecane. The generated droplets of n-tetradecane showed the highest degree of polydispersity. Our future work will be focused on the investigation of droplet generation at much higher oil flow rates through the plate, which is very important in practical applications.

5. List of Symbols

CV	coefficient of variation, -
$d_{4,3}$	volume-weighted mean particle diameter, m
$d_{3,2}$	mean Sauter particle diameter, m
$d_{channel}$	diameter of circular channels, m ($d_{channel} = 1 \times 10^{-5}$ m)
J_d	dispersed phase flux, m s^{-1}

k	fraction of active channels (N/N_0), -
N	number of active channels, -
N_0	total number of channels, -
Q_d	flow rate of disperse phase (oil) through MC plate, $m^3\ s^{-1}$
V_d	mean droplet volume, m^3
U	average velocity of oil inside circular channels, $m\ s^{-1}$
η_d	viscosity of dispersed phase (oil), Pa s
ν_{dg}	mean frequency of droplet generation, Hz

5. References

[1] Y. Hia, G. M. Whitesides, Soft lithography, *Annu. Rev. Mater. Sci.* 28 (1998) 153.

[2] S. Okushima, T. Nisisako, T. Torii, T. Higuchi, Controlled production of monodisperse double emulsions by two-step droplet breakup in microfluidic devices, *Langmuir* 20 (9905) 204.

[3] T. Kawakatsu, Y. Kikuchi, M. Nakajima, Regular-sized cell creation in microchannel emulsification by visual microprocessing method, *J. Am. Oil Chem. Soc.* 74 (1997) 317.

[4] L. Yobas, S. Martens, W.L. Ong, N. Ranganathan, High-performance flow-focusing geometry for spontaneous generation of monodispersed droplets, Lab Chip 6 (2006) 1073.

[5] J. Kameoka, H.G. Craighead, H.W. Zhang, J. Henion, A polymeric microfluidic chip for CE/MS determination of small molecules, *Anal. Chem.* 73 (2001) 1935.

[6] A. Hatch, A.E. Kamholz, K.R. Hawkins, M.S. Munson, E.A. Schilling, B.H. Weigl, P. Yager, A rapid diffusion immunoassay in a T-sensor, *Nature Biotechnology* 19 (2001) 461.

[7] H. Andersson, A. van den Berg, Microfluidic devices for cellomics: a review, *Sensors and Actuators B* 92 (2003) 315.

[8] D. Figeys, D. Pinto, Proteomics on a chip: Promising developments, *Electrophoresis* 22 (2001) 208.

[9] M.A. McClain, C.T. Culbertson, S.C. Jacobson, J.M. Ramsey, Flow cytometry of *Escherichia coli* on microfluidic devices, *Anal. Chem.* 73 (2001) 5334.

[10] I. Kobayashi, S. Mukataka, M. Nakajima, Production of monodisperse oil-in-water emulsions using a large silicon straight-through microchannel plate, *Ind. Eng. Chem. Res.* 44 (2005) 5852.

[11] S. Sugiura, M. Nakajima, H. Itou, M. Seki, Synthesis of polymeric microspheres with narrow size distributions employing microchannel emulsification, *Macromol. Rapid Commun.* 22 (2001) 77.

[12] S. Sugiura, M. Nakajima, M. Seki, Preparation of monodispersed emulsion with large droplets using microchannel emulsification, *J. Am. Oil Chem. Soc.* 79 (2002) 515.

[13] S. Iwamoto, K. Nakagawa, S. Sugiura, M. Nakajima, Preparation of gelatin microbeads with a narrow size distribution using microchannel emulsification, *AAPS PharmSciTech.* 3 (2002) article 25.

[14] F. Ikkai, S. Iwamoto, E. Adachi, M. Nakajima, New method of producing mono-sized polymer gel particles using microchannel emulsification and UV irradiation, *Colloid. Polym. Sci.* 283 (2005) 1149.

[15] S. Sugiura, M. Nakajima, J. Tong, H. Nabetani, M. Seki, Preparation of monodispersed solid lipid microspheres using a microchannel emulsification technique, *J. Colloid Interface Sci*. 227 (2000) 95.

[16] I. Kobayashi, Y. Iitaka, S. Iwamoto, S. Kimura and M. Nakajima, Preparation characteristics of lipid microspheres using microchannel emulsification and solvent evaporation methods, *J. Chem. Eng. Jpn.* 36 (2003) 996.

[17] K. Nakagawa, S. Iwamoto, M. Nakajima, A. Shono, Kazumi Satoh, Microchannel emulsification using gelatin and surfactant-free coacervate microencapsulation, *J. Colloid Interface Sci.* 278 (2004) 198.

[18] M, Yasuno, S. Sugiura, S. Iwamoto, M. Nakajima, A. Shono, K. Satoh, Monodispersed microbubble formation using microchannel technique, *AIChE J.* 50 (2004) 3227.

[19] T. Kuroiwa, S. Sugiura, M. Nakajima, S. Sato, S. Mukataka, S. Ichikawa, Preparation of giant vesicles with a controlled size and a high entrapment yield from monodisperse

emulsions, *6th European Symposium on Biochemical Engineering Science*, Salzburg, Austria, 27-30 August 2006.

[20] I. Kobayashi, K. Uemura, M. Nakajima, Controlled generation of monodisperse discoid droplets using microchannel arrays, *Langmuir* 22 (2006) 10893.

[21] Q. Xu, M. Nakajima, B.P. Binks, Preparation of particle-stabilized oil-in-water emulsions with the microchannel emulsification method, *Colloid. Surf. A* 262 (2005) 94.

[22] S. Sugiura, T. Oda, Y. Izumida, Y. Aoyagi, M. Satake, A. Ochiai, N. Ohkohchi, M. Nakajima, Size control of calcium alginate beads containing living cells using micro-nozzle array, *Biomaterials* 26 (2005) 3327.

[23] I. Kobayashi, M. Nakajima, K. Chun, Y. Kikuchi, H. Fujita, Silicon array of elongated through-holes for monodisperse emulsion droplets, *AIChE J.* 48 (2002) 1639.

[24] Y. Kikuchi, K. Sate, H. Ohki, T. Kaneko, Optically accessible microchannels formed in a single-crystal silicon substrate for studies of blood rheology, *Microvasc. Res.* 44 (1992) 226.

[25] I. Kobayashi, M. Nakajima, S. Mukataka, Preparation characteristics of oil-in-water emulsions using differently charged surfactants in straight-through microchannel emulsification, *Colloid. Surf. A* 229 (2003) 33.

[26] I. Kobayashi, S. Mukataka, M. Nakajima, Effects of type and physical properties of oil phase on oil-in-water emulsion droplet formation in straight-through microchannel emulsification, Experimental and CFD studies, *Langmuir* 21 (2005) 5722.

[27] I. Kobayashi, X. Lou, S. Mukataka, M. Nakajima, Preparation of monodisperse water-in-oil-in-water emulsions using microfluidization and straight-through microchannel emulsification, *J. Am. Oil Chem. Soc.* 82 (2005) 65.

[28] I. Kobayashi, S. Mukataka, M. Nakajima, Effect of slot aspect ratio on droplet formation from silicon straight-through microchannels, *J. Colloid Interface Sci.* 279 (2004) 277.

[29] I. Kobayashi, S. Mukataka, M. Nakajima, Novel asymmetric through-hole array microfabricated on a silicon plate for formulating monodisperse emulsions, *Langmuir* 21 (2005) 7629.

[30] Z. Nie, S. Xu, M. Seo, P.C. Lewis, E. Kumacheva, Polymer particles with various shapes and morphologies produced in continuous microfluidic reactors, *J. Am. Chem. Soc.* 127 (2005) 8058.

[31] A.S. Utada, E. Lorenceau, D.R. Link, P.D. Kaplan, H.A. Stone, D.A. Weitz, Monodisperse double emulsions generated from a microcapillary device, *Science* 308 (2005) 537.

[32] G.T. Vladisavljević, I. Kobayashi, M. Nakajima, R.A. Williams, M. Shimizu, T. Nakashima, Shirasu Porous Glass membrane: Characterisation of microstructure by high resolution x-ray microtomography and visualisation of droplet formation in real time, *J. Membr. Sci*, submitted.

[33] R.A. Williams, S.J. Peng, D.A. Wheeler, N.C. Morley, D. Taylor, M. Whalley and D.W. Houldsworth, Controlled Production of Emulsions Using a Crossflow Membrane Part II: Industrial Scale Manufacture, *Chem. Eng. Res. Des*. 76A (1998) 902-910.

[34] G.T. Vladisavljević, U. Lambrich, M. Nakajima, H. Schubert, Production of O/W emulsions using SPG membranes, ceramic α-aluminium oxide membranes, microfluidizer and a silicon microchannel plate – a comparative study, *Colloid. Surf. A* 232 (2004) 199.

[35] I. Kobayashi, K. Uemura, M. Nakajima, CFD study of the effect of a fluid flow in a channel on generation of oil-in-water emulsion droplets in straight-through microchannel emulsification, *J. Chem. Eng. J.* 39 (2006) 855.

[36] Y.C. Tan, V. Cristini, A.P. Lee, Monodispersed microfluidic droplet generation by shear focusing microfluidic device, *Sensor. Actuat. B-Chem.* 114 (2006) 350.

[37] S.L. Anna, N. Bontoux, H.A. Stone, Formation of dispersions using “flow focusing” in microchannels, *Appl. Phys. Lett.* 82 (2003) 364.

[38] X. Zhang, Dynamics of drop formation in viscous flows, *Chem. Eng. Sci.* 54 (1999) 1759.

[39] X.D. Shi, M.P. Brenner, S.R. Nagel, A cascade of structure in a drop falling from a faucet, *Science* 265 (1994) 219.

[40] D.M. Henderson, W.G. Pritchard, L.B. Smolka, On the pinch-off of a pendant drop of viscous fluid, *Phys. Fluids* 9 (1997) 3188.

[41] Y.C. Tan, J.S. Fisher, A.I. Lee, V. Cristini, A.P. Lee, Design of microfluidic channel geometries for the control of droplet volume, chemical concentration, and sorting, *Lab Chip* 4 (2004) 292.

[42] Y.C. Tan, A.P. Lee, Microfluidic filtering and sorting of satellite droplets as the basis of a monodispersed micron and submicron emulsification system, *Lab Chip* 5 (2005) 1178.

[43] I. Kobayashi, G.T. Vladisavljević, K. Uemura, M. Nakajima, High-performance production of monodisperse emulsions using microfabricated asymmetric through-hole array, *The 11th International Conference on Miniaturized Systems for Chemistry and Life Sciences*, Paris, October 2007.

[44] G.T. Vladisavljević, H. Schubert, Influence of process parameters on droplet size distribution in SPG membrane emulsification and stability of prepared emulsion droplets, *J. Membr. Sci.* 225 (2003) 15.

[45] G.T. Vladisavljević, H. Schubert, Preparation of emulsions with a narrow particle size distribution using microporous α-alumina membranes, *J. Disper. Sci. Technol.* 24 (2003) 811.

Acknowledgement.

Goran Vladisavljević sincerely thanks the Japan Society for the Promotion of Science, Tokyo (The Invitation fellowship ID No. L-05555) for the financial support of this work. This work was also supported financially by the Food Nanotechnology Project of the Ministry of Agriculture, Forestry and Fisheries of Japan.

Tables

Table 1. Geometric characteristics of the WMS1-3 microchip

Dimensions of microslots	10×50 μm
Diameter of circular microchannels	10 μm
Depth of microslots	30 μm
Length of circular microchannels	70 μm
Total length of asymmetric microchannels	100 μm
Total number of channels, N_0	$142 \times 83 + 141 \times 83 = 23{,}489$
Active cross-sectional area of microchip	10×10 mm
Total cross-sectional area of microchip	24×24 mm

Table 2. Properties of dispersed phase (oils) used in this work

oil	density at 25 °C kg/m^3	viscosity at 25 °C mPa·s	refractive index	interfacial tension* mN/m
soybean oil	920	50	1.47	25
n-tetradecane	763	2.7	1.43	50
MCT oil**	940	20	1.45	30

*In contact with pure water.

**MCT = Medium-chain triglyceride

Table 3. Effect of oil type on droplet generation for 2 wt% Tween 20 at Q_d = 1 mL h^{-1} (J_d = 10 L $m^{-2}h^{-1}$) and Q_c = 250-400 mL h^{-1} (SO = soybean oil, MCT = MCT oil, TD = n-tetradecane)

	$d_{4,3}$ μm	CV* %	span -	ν_{dg} Hz	N -	k %	U mm s^{-1}
SO	25.60	7.49	0.218	2.8	11,293	48.1	0.3
MCT	27.51	7.78	0.216	11.6	2,197	9.4	1.6
TD	28.01	16.1	0.491	25.8	936	4.0	3.8

*Measured using the light scattering instrument. The CV of droplet diameters for SO and MCT estimated from microscopic images using the WinRoof image analysis software was 3-4 %.

Figures

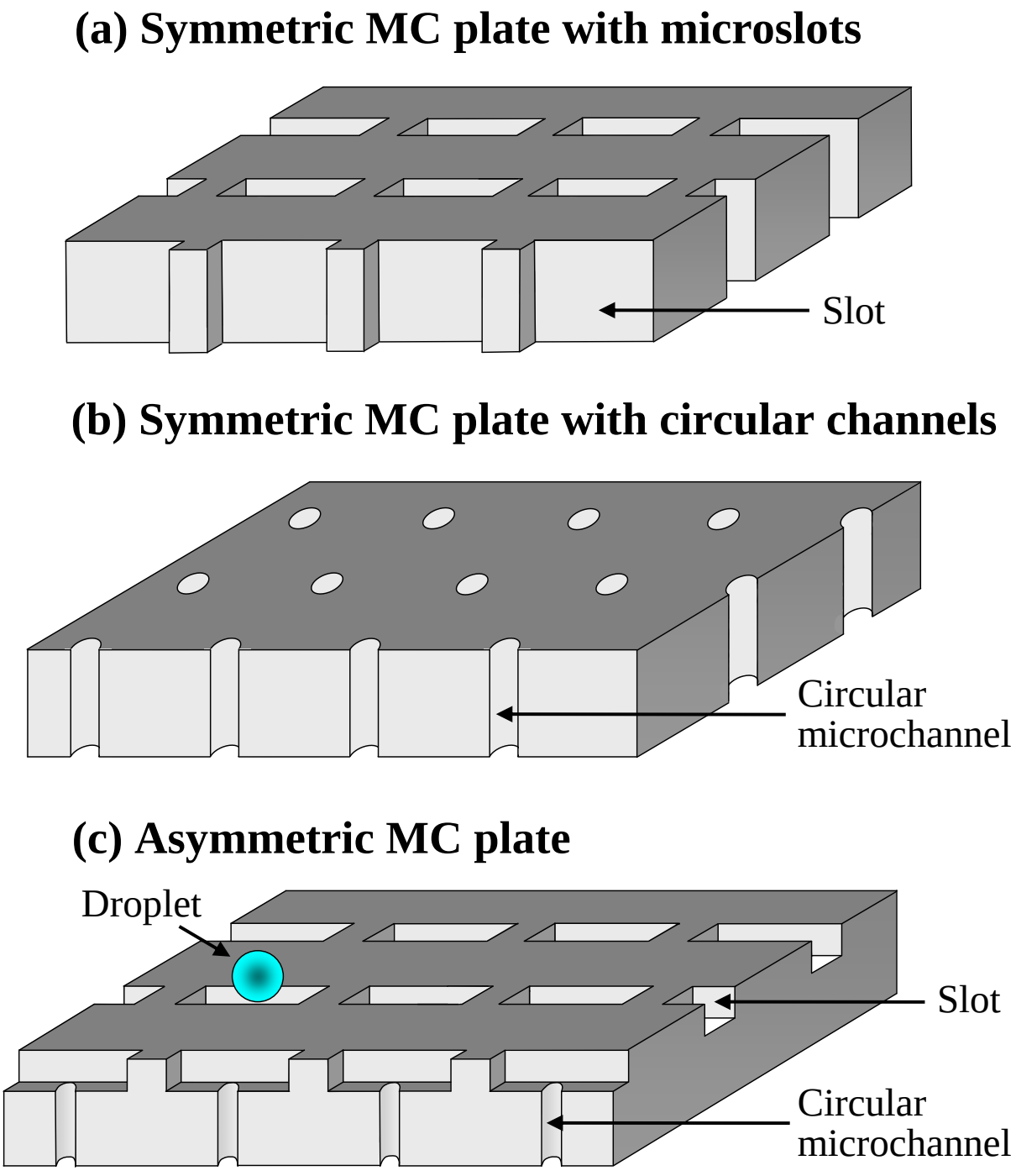

Figure 1: Schematic representation of symmetric and asymmetric microchannel plates.

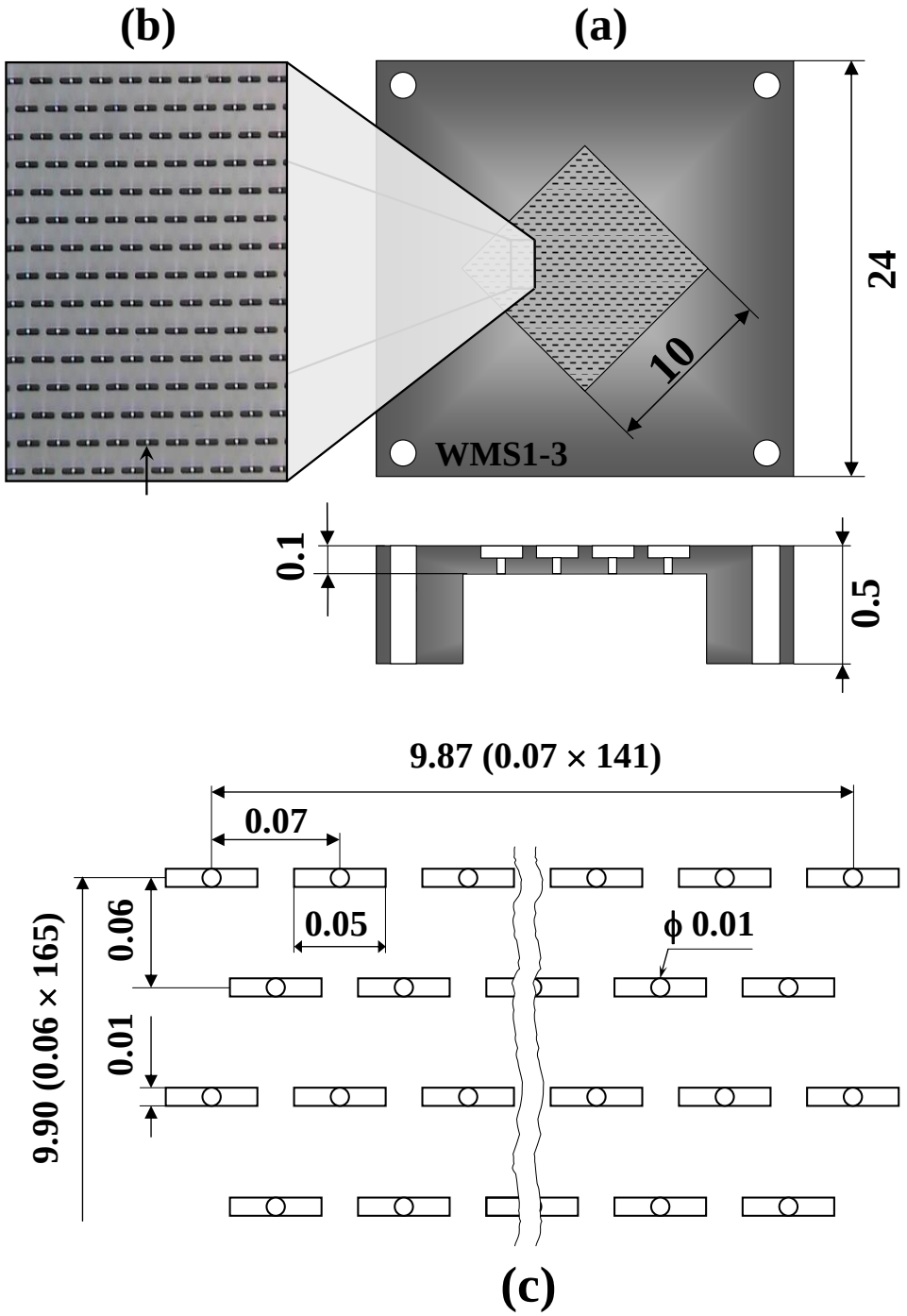

Figure 2. (a) Schematic representation of the WMS1-3 silicon chip; (b) Micrograph of the bottom-illuminated chip surface. The circular channels are visible as bright dots (see arrow) at the centre of each microslot; (c) Arrangement of channels on the top side of a WMS1-3 chip. Each horizontal row contains alternately 142 or 141 channels and there are overall 166 horizontal rows on the whole chip. All dimensions are in millimetres.

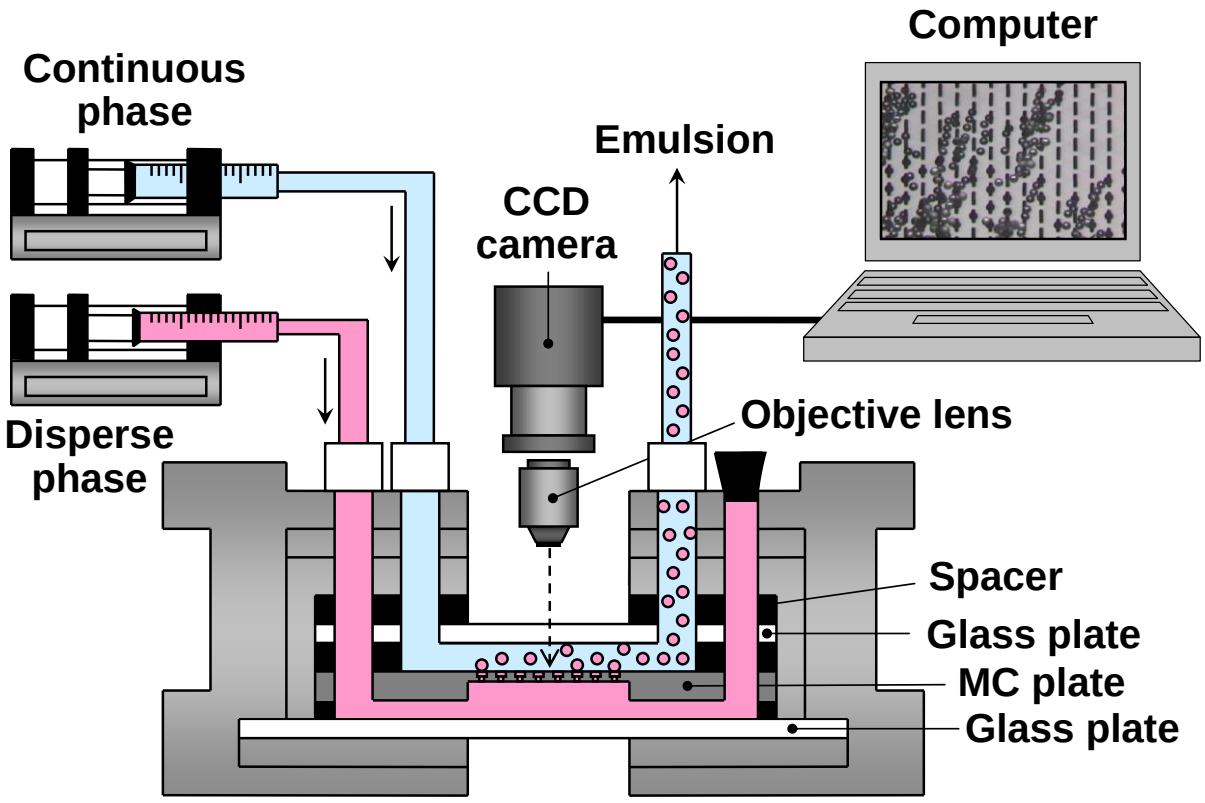

Figure 3. Simplified schematic of the experimental set-up used in this work for microchannel emulsification.

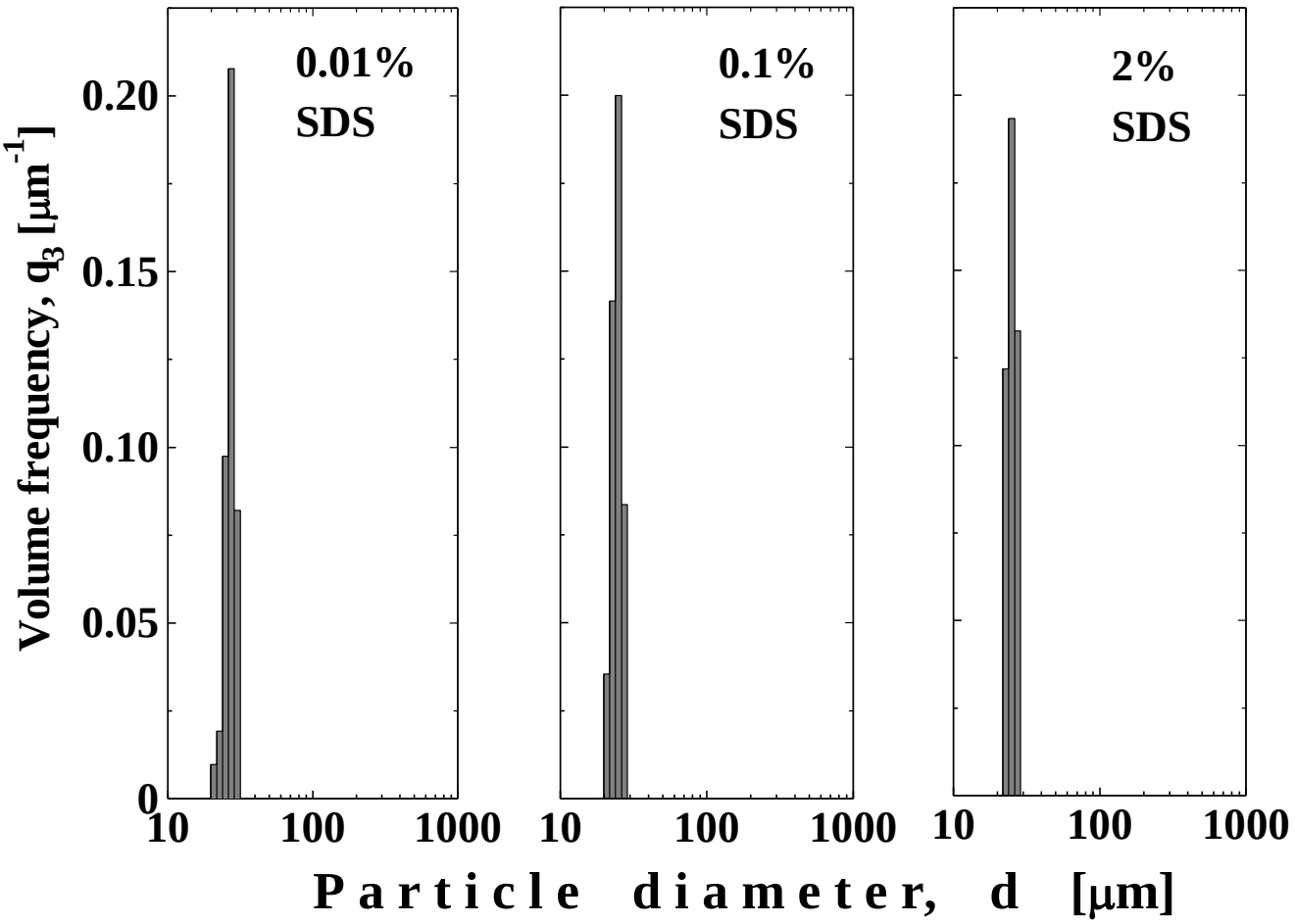

Figure 4. Particle size distribution of the generated soybean oil droplets at the constant oil flux of 10 $Lm^{-2}h^{-1}$ for three different concentrations of SDS (at 0.01 wt% SDS: $d_{3,2}$ = 29.0 μm and span = 0.225; at 0.1 wt% SDS: $d_{3,2}$ = 26.8 μm and span = 0.222; at 2 wt% SDS: $d_{3,2}$ = 26.3 μm and span = 0.213).

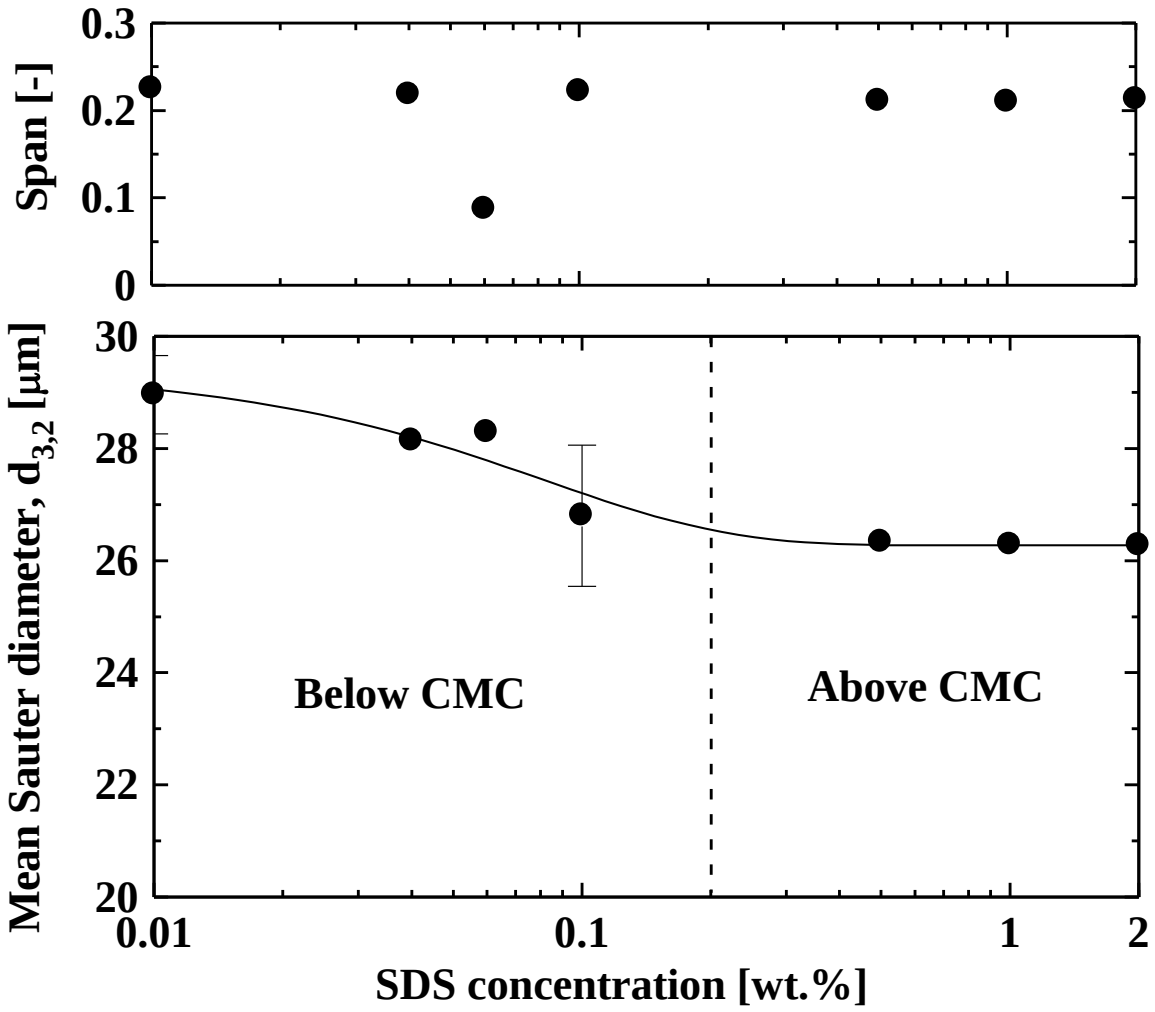

Figure 5. Effect of SDS concentration in the aqueous phase on the mean size of soybean oil droplets at $J_d = 10\ Lm^{-2}\ h^{-1}$.

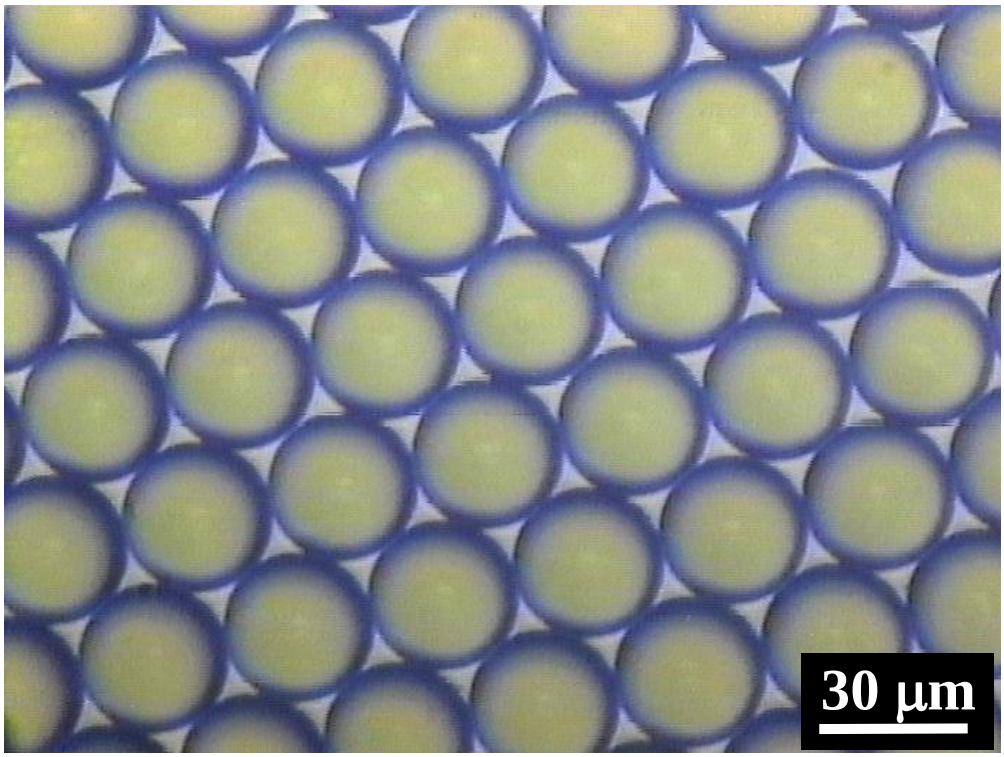

Figure 6. Micrograph of the resultant emulsion droplets prepared at the SDS concentration of 0.2 wt% and J_d = 10 $Lm^{-2}h^{-1}$.

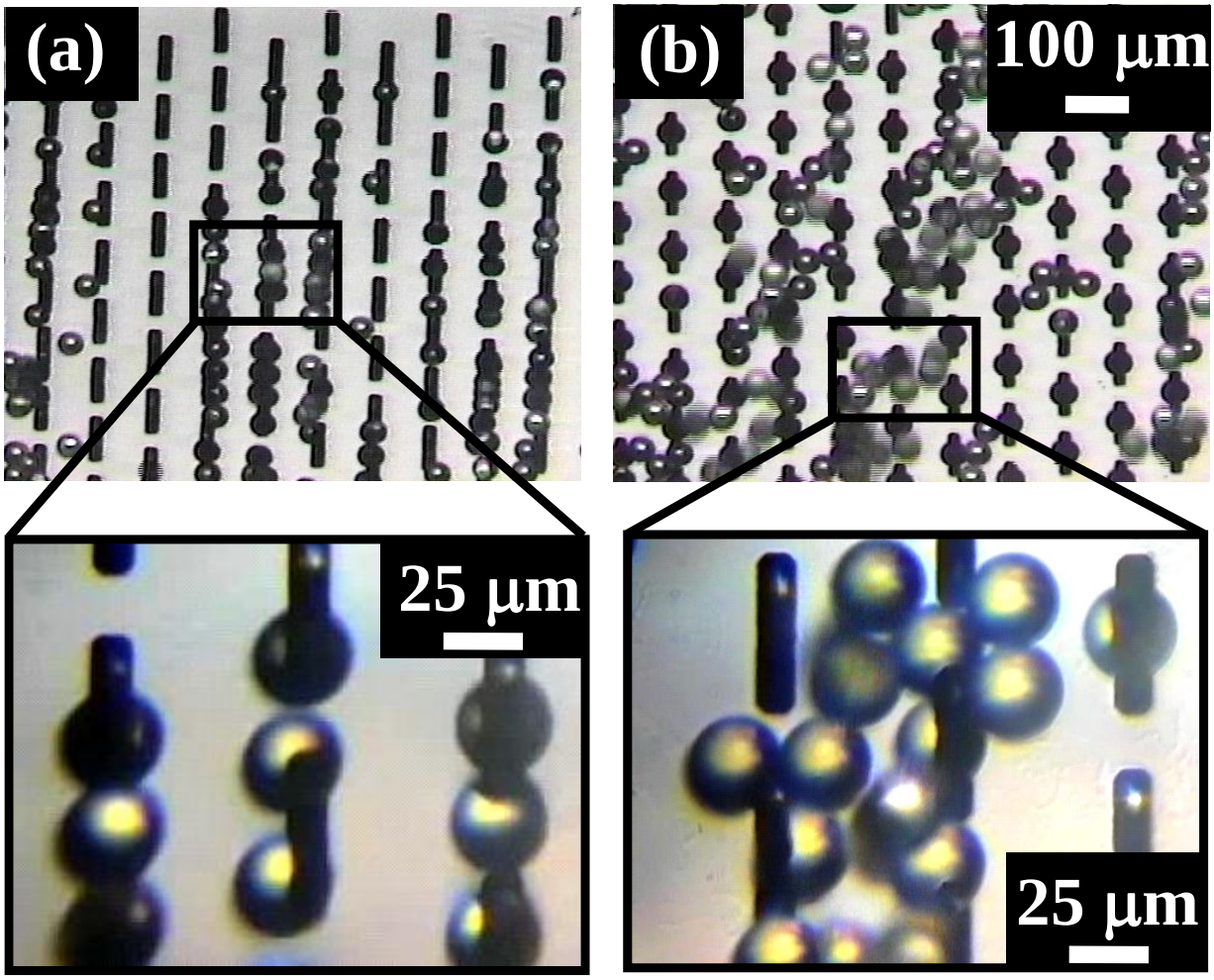

Figure 7. (a) Generation of soybean oil droplets at high SDS content (1 wt%). The droplets are detached from the plate surface as soon as they are formed; (b) Generation of soybean oil droplets at low (0.08 wt%) SDS content. The droplets are kept attached at the channel outlets, fixed to the plate surface by the high interfacial tension force.

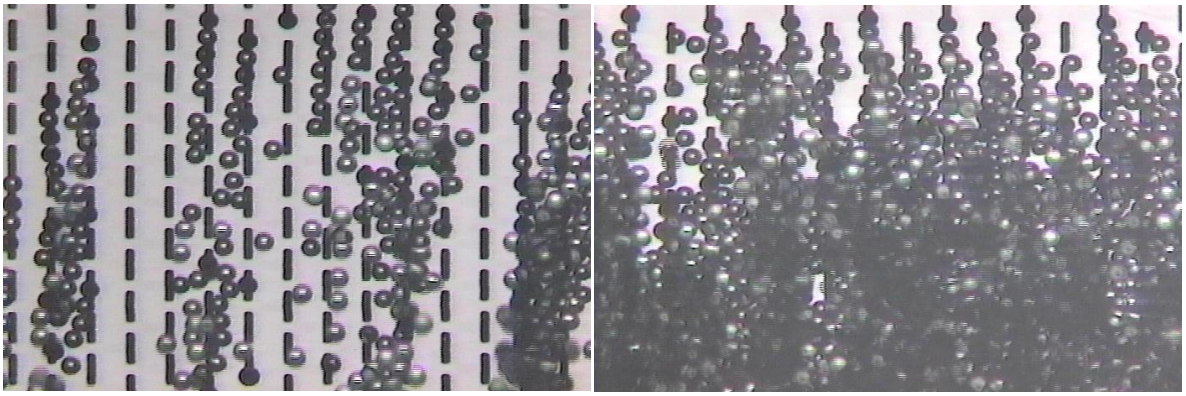

Figure 8. Formation of soybean oil droplets at 0.01 wt% SDS from different portions of the plate surface in the same experiment. It shows a significant variation of the percents of active channels over the plate surface at the high interfacial tension.

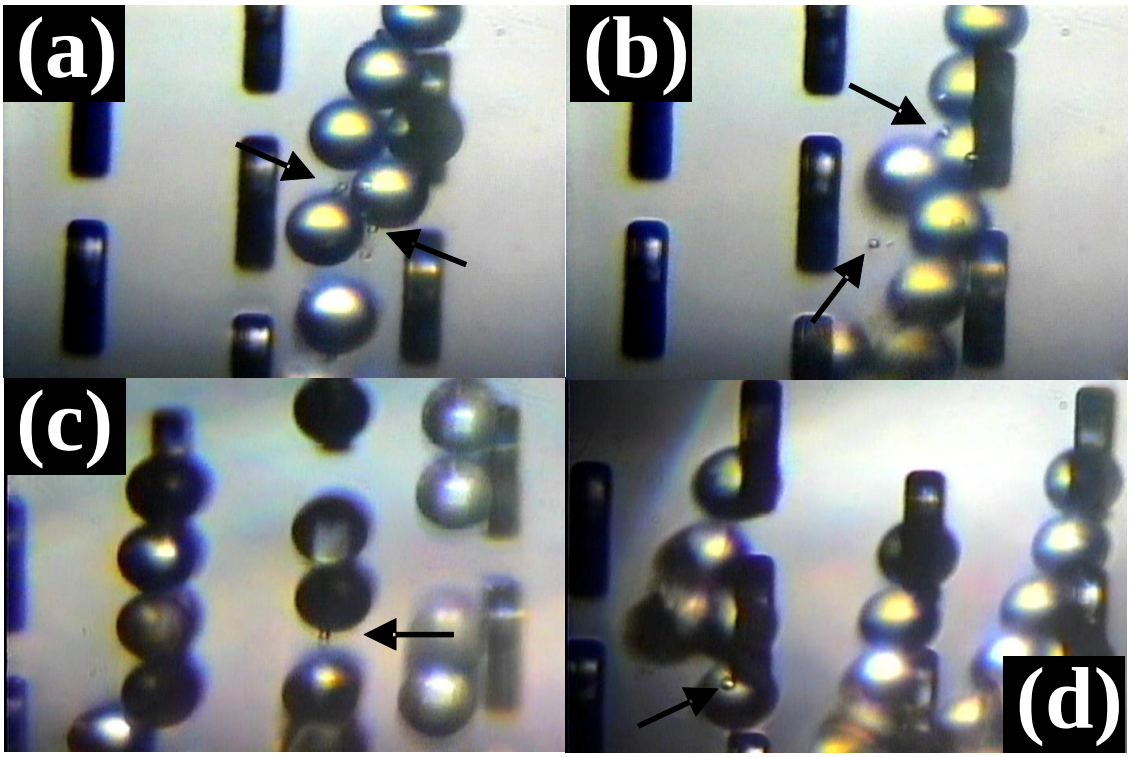

Figure 9. Formation of small satellite soybean oil droplets at 1 wt% SDS. The small droplets are marked by arrows.

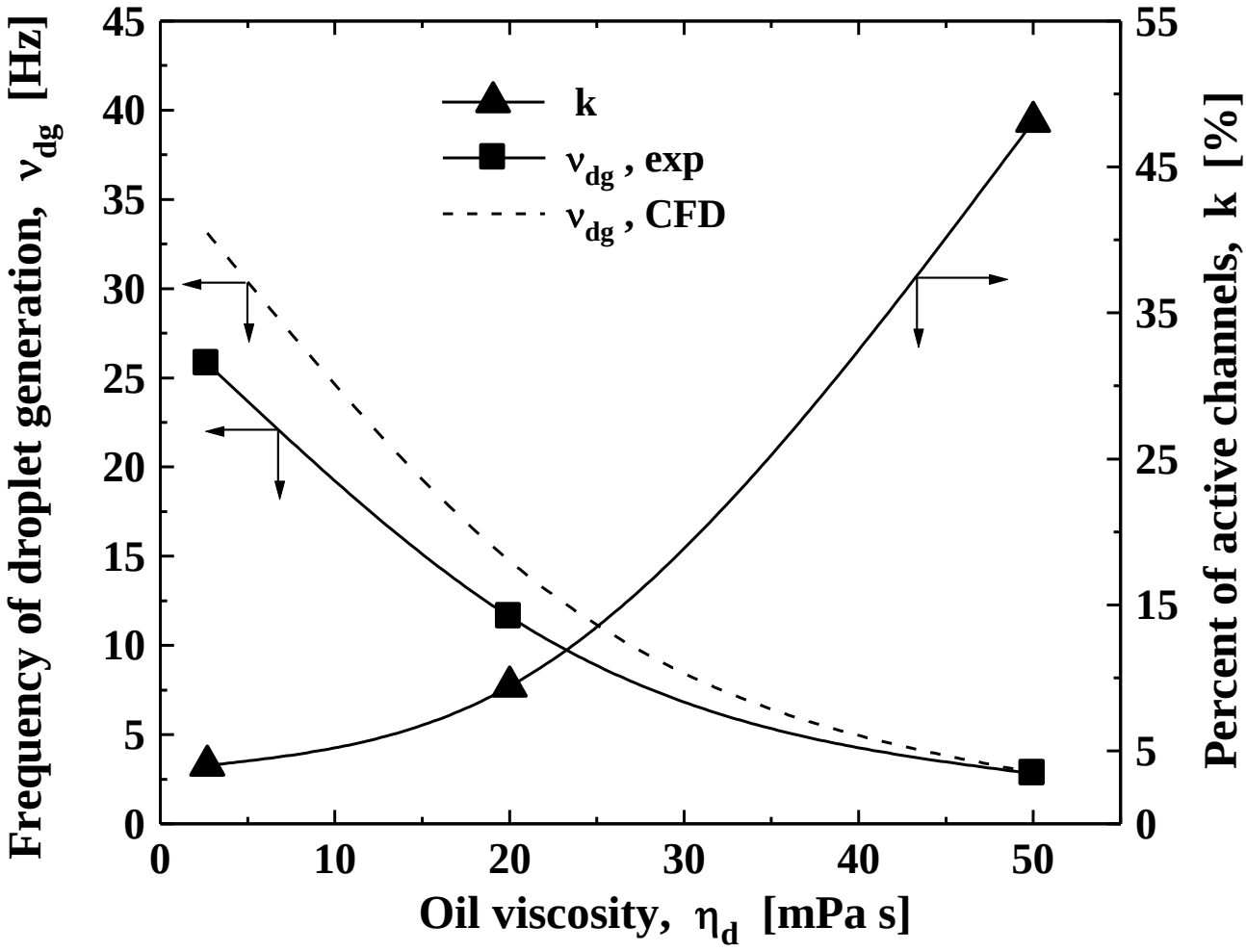

Figure 10. Frequency of droplet generation and percent of active channels as a function of oil viscosity for 2 wt% Tween 20 at J_d = 10 $Lm^{-2}h^{-1}$. The frequency of droplet generation vs. oil viscosity curve obtained by CFD simulation is shown by a dashed line.